

ON THE STABILITY OF A SELF-GRAVITATING INHOMOGENEOUS FLUID IN THE FORM OF TWO CONFOCAL SPHEROIDS ROTATING WITH DIFFERENT ANGULAR VELOCITIES

J. U. Cisneros Parra,¹ F. J. Martínez Herrera,² and J. D. Montalvo Castro²

Received 2000 June 9; accepted 2000 September 19

RESUMEN

Mediante la técnica del virial a segundo orden se analiza a primera aproximación la estabilidad de un fluido inhomogéneo autogravitante compuesto de dos esferoides confocales con rotación diferencial. Tal modelo tiene por solución de equilibrio una serie la que según el presente estudio es, casi en su totalidad, estable. Por otro lado, la serie contiene algunos esferoides de frecuencia natural cero, lo cual es un indicio de que de ellas pudiesen ramificarse secuencias de figuras triaxiales. De hecho, tal ramificación efectivamente se da, si bien hay que acotar que los elipsoides así bifurcados son tipo Dedekind, pues son estáticos con corrientes internas de vorticidades diferentes. El que (dado el modelo del cual se desprenden) dichas secuencias no consistan de elipsoides tipo Jacobi no debe sin embargo sorprender, si se atiende al teorema de Hamy.

ABSTRACT

The second order virial equations are employed to analyze in a first approximation the stability of a self-gravitating fluid made up of two confocal spheroids with solid-body differential rotation. The equilibrium solution for such a model is known to consist of a series which in the present study is shown to be, almost throughout, stable. On the other hand, the series contains some spheroids of zero frequency, an indication that secondary sequences of tri-axial figures could branch off from them. Such is indeed the case, even if the bifurcated sequences consist exclusively of Dedekind-type figures, as they are static with internal motions of differential vorticity. Anyway, Jacobi-type figures could not beforehand be expected to give out from the model, since it would be inconsistent with Hamy's theorem.

Key Words: GRAVITATION — HYDRODYNAMICS — STARS: ROTATION

1. INTRODUCTION

In relation to a past paper (Montalvo, Martínez, & Cisneros 1983) on the hydrostatic relative equilibrium of a self-gravitating, perfect, incompressible, fluid made up of two confocal spheroids with solid-body differential rotation we recall that, provided the internal spheroid (the “nucleus”) is of higher density and rotates faster than the external spheroid (the “atmosphere”), such a model satisfies the equilibrium conditions. A specific configuration i.e., an equilibrium figure, is determined by giving the body's relative density $\varepsilon [= (\rho_n - \rho_a)/\rho_a]$, where ρ is the density, along with specifying the angular velocity of solid-body rotation around the $x_3 - axis$, ω , and the meridional eccentricity, ϵ , of each of its two composing spheroids.

In our case, the confocality condition is assumed to simplify the algebra (but see, however, the reasons for confocality given by Chambat 1994). As the complete equilibrium solution of this Maclaurin-type model spans through a continuum of the parameters that describe it, following the standard literature on the subject we

¹Facultad de Ciencias, Universidad Autónoma de San Luis Potosí, México.

²Instituto de Física, Universidad Autónoma de San Luis Potosí, México.

refer to it as a “series”. For equilibrium figures to exist it is then required $\omega_n > \omega_a$ which, in addition, must be of $\epsilon_n > \epsilon_a$ by confocality. The case $\omega_n = \omega_a$ admits no equilibrium solution (Tassoul 1978; Montalvo et al. 1983). It is worth to mention here that our model does not work for ellipsoids, neither for $\omega_n = \omega_a$, nor for $\omega_n \neq \omega_a$. The first case is contemplated by Hamy’s theorem (Hamy 1887), which states that no stratification made up of *any number* of confocal ellipsoids rotating, all with the same angular velocity, is an equilibrium figure. For the second case we have no reference but, *a priori*, its impossibility looks sound if one considers, as a plausible argument, that the interaction between the field velocities of the nosses of the body’s two ellipsoids would induce unwanted dynamical effects. On the other hand, we know (Cisneros, Martínez, & Montalvo 1995) that inhomogeneous Dedekind-type figures both, spheroidal and ellipsoidal, are equilibrium figures in the event that they have an internal motion of differential vorticity (no equilibrium solution exists for the common vorticity case). This result is, in connection with the current problem, independently recovered—with a much higher degree of accuracy than in 1995—and is of fundamental importance for our present conclusions. With this scenario it is, therefore, natural to ask if a stability (actually, dynamical stability, as frictional effects will be ignored) analysis—here carried out by means of the virial technique—of the inhomogeneous spheroidal series, which is the purpose of the current paper, could account for the interrelation of the above results, and afford some ideas, however crude, about the evolution of our model.

We will see that, at least qualitatively, our relatively simple analysis yields results that bear a resemblance with more involved ones. Nevertheless, the model contains an element of truth namely that, as in the evolution of real stars, the cores become denser and denser, and therefore rotate faster and faster than their envelopes. Regardless that the current work was originally planned to be carried out for its own sake, it would seem, *a posteriori*, that such interest may be of astrophysical character.

2. THE VIRIAL METHOD

The well-known results on the equilibrium and the stability of the various classic ellipsoidal series (Maclaurin’s, Jacobi’s, Dedekind’s, etc.) have been recovered in the 1960’s, by means of the virial method, in a series of individual papers by Chandrasekhar & Lebovitz (1962), a work that was later recopiled by the first in a book (Chandrasekhar 1969; hereafter, Ch 1969); in particular, the analysis of the stability of the Maclaurin figures was made using a non-inertial frame of reference. Meanwhile, the virial theory which, as regards to fluids is not restricted to homogeneous masses, was applied to a centrally condensed axial symmetric compressible rotating fluid (Tassoul & Ostriker 1968; hereafter, T&O). T&O’s approach was achieved with respect to an inertial frame of reference, which fits well to our model of differential rotation, and so will be closely followed here.

The incompressible character of our fluid will be handled as explained in § 2.3.3. In essence, the virial method consists in replacing the equation of motion governing a problem by its moments with respect to the coordinates. Thus to second order—the current approximation—the virial equations are obtained by multiplying the j component of the equation of motion by x_i , followed by an integration over the volume instantaneously occupied by the fluid. The resulting equation is then slightly disturbed by means of a Lagrangian displacement $\vec{\xi}(\vec{x}, t)$, which in a first approximation, can be given by $\xi_i = L_{i;j}x_k$, where $L_{i;k}$ denotes nine constants. Let

$$\vec{\xi}(\vec{x}, t) = \vec{\xi}(\vec{x})e^{\lambda t}, \quad (1)$$

be the time dependence of the perturbation, where λ is a characteristic value. We may formally initiate our analysis by deriving an equation similar, at any rate, to T&O’s equation (23), here reproduced as a quick reference as equation (2)

$$\begin{aligned} & \lambda^2 L_{i;j} \int_V \rho x_j x_j dV - 2\lambda L_{i;k} \int_V \rho Q_{jk} x_k x_k dV \\ & + L_{i;k} \int_V \rho Q_{jk}^2 x_k x_k dV + L_{j;k} \int_V \rho Q_{ik}^2 x_k x_k dV \\ & = -L_{ks} W_{sk;ij} + \delta_{ij} L_{k;k} P, \end{aligned} \quad (2)$$

where

$$\mathbf{W}_{sk;ij}(x) = \int_V \rho x_s \partial \mathbf{B}_{ij}(x) / \partial x_k dV, \quad (3)$$

and

$$\mathbf{B}_{ij} = G \int_V \rho(x') \frac{(x_i - x'_i)(x_j - x'_j)}{|\vec{x} - \vec{x}'|^3} dV. \quad (4)$$

Now, equation (4) gives the tensor of potential energy \mathbf{B}_{ij} , so that equation (3), which depends on four, rather than two indices is usually called the supertensor of potential energy, which first pair of indices refers to the coordinates x while the second one to the tensor \mathbf{B}_{ij} (Chandrasekhar & Lebovitz 1962). In equation (2) summation over repeated indices is understood. If the changes in pressure, accompanying the changes in density, take place adiabatically, then the change in pressure is given by

$$P = - \int_V (\Gamma - 1) pdV. \quad (5)$$

Orienting Ω along the $x_3 - axis$, the components of the velocity u of any point x_j of the fluid are given by

$$u_i(x) = Q_{ij}(\bar{\omega})x_j, \quad (6)$$

where Q_{ij} is a matrix of nine elements, of which $Q_{12} = -1$, $Q_{21} = +1$ and zero otherwise; also

$$Q_{ij}^2 = Q_{ik}Q_{kj}. \quad (7)$$

The definitions concerning the average of the angular velocity are

$$\langle \Omega \rangle = \int_V \Omega(\bar{\omega})\bar{\omega}^2 \rho(x) dx / \int_V \bar{\omega}^2 \rho(x) dx, \quad (8)$$

and

$$\langle \Omega^2 \rangle = \int_V \Omega^2(\bar{\omega})\bar{\omega}^2 \rho(x) dx / \int_V \bar{\omega}^2 \rho(x) dx. \quad (9)$$

We need now to extend the above definitions so as to fit into our model and to realize that, since ours is an incompressible fluid, eventually the change in pressure (5) will be eliminated from the equations and the remaining equations will be supplemented by the conditions that follow from the requirement that in this case only displacements which are divergence free should be considered (Ch 1969). Such elimination will be explicitly performed in § 2.3.

2.1. The Volume Integrals

The volume integrals in equation (2) are meant to be carried out over the volume occupied by the whole body namely, $V = V_n + V_a$, so that for one such integral we may write, say,

$$\int_V \rho dV \rightarrow \int_{V_n} \rho_n dV + \int_{V_a} \rho_a dV.$$

Next, the last integral is splitted into two as suggested by Figure 1, that is,

$$\begin{aligned} \int_V \rho dV &\rightarrow \int_{V_n} \rho_n dV + \int_V \rho_a dV \\ &\quad - (\varepsilon + 1)^{-1} \int_{V_n} \rho_n dV, \end{aligned} \quad (10)$$

where the factor $(\varepsilon + 1)^{-1}$ in the last integral compensates the excess of density implied in the penultimate one, and turns it into an integral with the volume and density of the nucleus.

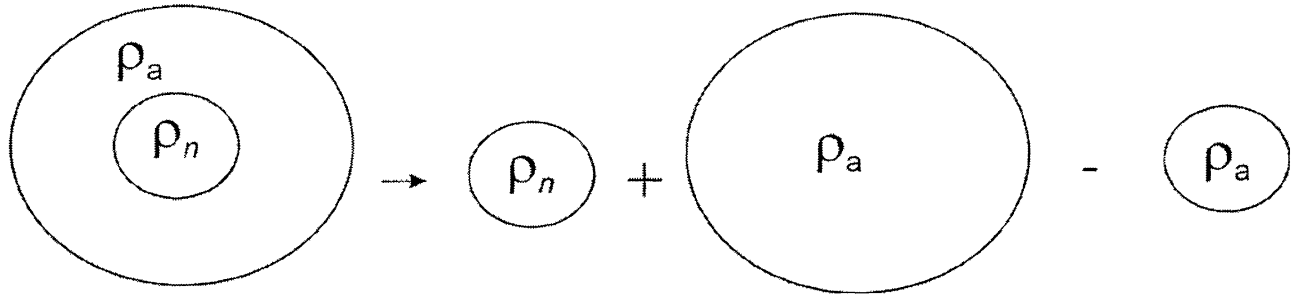


Fig. 1. The volume integrals needed for equation (11) can be taken from equation (2) if the last are splitted as suggested by this scheme.

Proceeding in this way over both sides of equation (2) there results

$$\begin{aligned}
 & \lambda^2 [L_{i;j} \int_{V_n} \rho_n x_j x_j dV + L_{i;j} \int_V \rho_a x_j x_j dV - (\varepsilon + 1)^{-1} L_{i;j} \int_{V_n} \rho_n x_j x_j dV] \\
 & - 2\lambda [L_{i;k} \int_{V_n} \rho_n Q_{jk}^n x_k x_k dV + L_{i;k} \int_V \rho_a Q_{jk}^a x_k x_k dV - (\varepsilon + 1)^{-1} L_{i;j} \int_{V_n} \rho_n Q_{jk}^a x_k x_k dV] \\
 & + L_{i;k} \int_{V_n} \rho_n (Q_{jk}^n)^2 x_k x_k dV + L_{i;k} \int_V \rho_a (Q_{jk}^a)^2 x_k x_k dV - (\varepsilon + 1)^{-1} L_{i;k} \int_{V_n} \rho_n (Q_{jk}^a)^2 x_k x_k dV \\
 & + L_{j;k} \int_{V_n} \rho_n (Q_{ik}^n)^2 x_k x_k dV + L_{j;k} \int_V \rho_a (Q_{ik}^a)^2 x_k x_k dV - (\varepsilon + 1)^{-1} L_{j;k} \int_{V_n} \rho_n (Q_{ik}^a)^2 x_k x_k dV \\
 & = -2\pi G \rho_a * \{ B_{ij}^a L_{k;s} \int_{V_n} \rho_n (x_i x_s \delta_{jk} + x_j x_s \delta_{ik}) dV - a_{a_i}^2 A_{ik}^a L_{k;s} \int_{V_n} \rho_n x_k x_s \delta_{ij} dV \\
 & + \varepsilon [B_{ij}^n L_{k;s} \int_{V_n} \rho_n (x_i x_s \delta_{jk} + x_j x_s \delta_{ik}) dV - a_{n_i}^2 A_{ik}^n L_{k;s} \int_{V_n} \rho_n x_k x_s \delta_{ij} dV] \\
 & + B_{ij}^a L_{k;s} \int_V \rho_a (x_i x_s \delta_{jk} + x_j x_s \delta_{ik}) dV - a_{a_i}^2 A_{ik}^a L_{k;s} \int_V \rho_a x_k x_s \delta_{ij} dV \\
 & + \varepsilon [B'_{ij}^n L_{k;s} \int_V \rho_a (x_i x_s \delta_{jk} + x_j x_s \delta_{ik}) dV - a_{n_i}^2 A'_{ik}^n L_{k;s} \int_V \rho_a x_k x_s \delta_{ij} dV] \\
 & - (\varepsilon + 1)^{-1} [B_{ij}^a L_{k;s} \int_{V_n} \rho_n (x_i x_s \delta_{jk} + x_j x_s \delta_{ik}) dV - a_{a_i}^2 A_{ik}^a L_{k;s} \int_{V_n} \rho_n x_k x_s \delta_{ij} dV] \\
 & + \varepsilon [B'_{ij}^n L_{k;s} \int_{V_n} \rho_n (x_i x_s \delta_{jk} + x_j x_s \delta_{ik}) dV - a_{n_i}^2 A'_{ik}^n L_{k;s} \int_{V_n} \rho_n x_k x_s \delta_{ij} dV]] \} \\
 & - L_{k;k} \int_{V_n} (\Gamma - 1) p_n \delta_{ij} dV - L_{k;k} \int_V (\Gamma - 1) p_a \delta_{ij} dV + L_{k;k} \int_{V_n} (\Gamma - 1) p_a \delta_{ij} dV . \tag{11}
 \end{aligned}$$

The various quantities in equation (11) are no more than the definitions (3) to (9) extended to our model, which present no difficulty, except for excessive writing; they will be given as we proceed onwards.

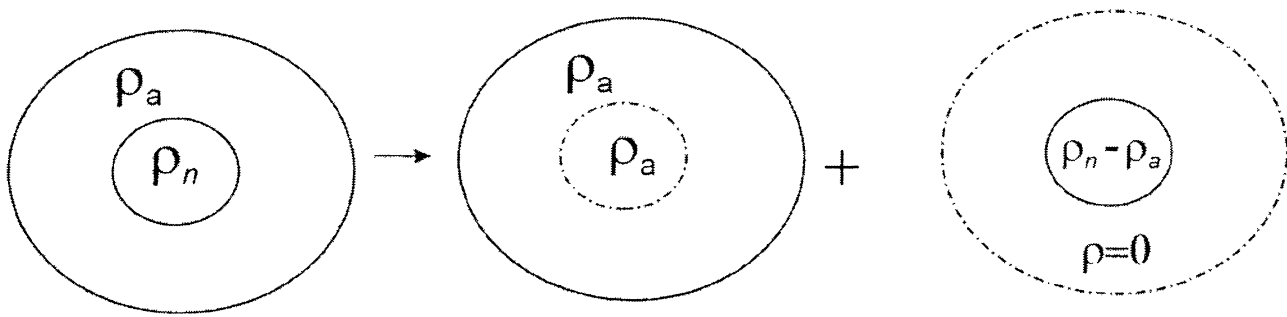


Fig. 2. Illustrating the artifice used to take into account the inhomogeneous character of the tensor of potential energy in the evaluation of the supertensor of potential energy.

The L_{ij} 's in equation (11) have not been labeled with a superscript n or a because, for ease of calculation, these quantities are assumed continuous across the border between the nucleus and the atmosphere where, in addition, the potential—and so the pressure—is continuous (Landau & Lifshitz 1959). The corresponding nine equations following from equation (11) are written at length in § 2.3.1. The evaluation of the supertensor of potential energy will be considered in the next section.

2.2. Evaluation of the Supertensor of Potential Energy

From the properties (Chandrasekhar & Lebovitz 1962) of the supertensor of potential energy, equation (3), we know that only twenty one of its elements are nonvanishing and that, upon using the symmetry property of its second pair of indices, this number can be reduced to fifteen, they being

$$\mathbf{W}_{31;13}, \mathbf{W}_{13;13}, \mathbf{W}_{32;23}, \mathbf{W}_{23;23}, \mathbf{W}_{11;11}$$

$$\mathbf{W}_{22;11}, \mathbf{W}_{33;11}, \mathbf{W}_{11;22}, \mathbf{W}_{22;22}, \mathbf{W}_{33;22}$$

$$\mathbf{W}_{11;33}, \mathbf{W}_{22;33}, \mathbf{W}_{33;33}, \mathbf{W}_{21;12}, \mathbf{W}_{12;12} .$$

Let us consider the evaluation of one of these single terms for our model. After splitting according to equation (10) the integral in equation (3) we have still to deal with the inhomogeneous character of its integrand—namely the tensor of potential energy \mathbf{B}_{ij} —in view of its dependence on points of both the nucleus and the atmosphere. To derive the total tensor of potential energy of the atmosphere, we follow the steps depicted in Figure 2.

Thus the total tensor of potential energy consists of two contributions: one, resulting from the interior of a volume occupied by the whole body, supposed of density ρ_a throughout, plus another, resulting from the exterior of a volume occupied only by the nucleus, supposed of density $\rho_n - \rho_a$ to compensate the excess of mass implied in the first contribution. We thus have

$$\mathbf{B}_{ij}(x_a) = \mathbf{B}_{ij}^{int.}(x_a) + \mathbf{B}_{ij}^{ext.}(x_a) , \quad (12)$$

and it follows that the total tensor of potential energy of the nucleus is the sum of two interior contributions.

The expression for the supertensor of potential energy is then

$$\begin{aligned} \mathbf{W}_{sk;ij} = & \int_{V_n} \rho_n x_s \partial \mathbf{B}_{ij}(x_n) / \partial x_k dV \\ & + \int_{V_a} \rho_a x_s \partial \mathbf{B}_{ij}(x_a) / \partial x_k dV . \end{aligned} \quad (13)$$

Now, the expression for \mathbf{B}_{ij} at an interior point of a homogeneous ellipsoid is given by

$$\mathbf{B}_{ij}^{int.} = \pi G \rho * [2B_{ij} x_i x_j + a_i^2 \delta_{ij} (A_i - \sum_{l=1}^3 A_{il} x_l^2)]^{int.}, \quad (14)$$

where A_i , A_{il} , B_{ij} are the so called index symbols, a_i are the semiaxes of the ellipsoid, and G is the gravitational constant. The index symbols are elliptic integrals running from 0 (λ) to ∞ if we are to compute interior (exterior) contributions to \mathbf{B}_{ij} , where λ is the ellipsoidal coordinate of the considered point (Ch 1969). The meaning of the various terms in equation (11) is now clear where, in addition, the following properties apply: $a_1 = a_2 > a_3$; the moments of inertia I_{ij} referring to the whole body are designated by a superscript b , and $I_{11} = I_{22}$; the $\mathbf{W}_{sk;ij}$'s are normalized to $\pi G \rho_a$; the symmetry of the index symbols requires that, for example, $B_{21} = B_{12} = B_{11}$, those symbols referring to interior (exterior) contributions to the tensor \mathbf{B}_{ij} being designated by the usual capital undashed (dashed) letters.

2.3. The Dispersion Relations

Sustituting $\sigma = -i\lambda$, where σ is the frequency, in the nine equations derived from equation (11), a dispersion relation in the frequency can be obtained for each of three different modes of oscillation: transverse-shear, toroidal, and pulsation, where Chandrasekhar's nomenclature has been preferred over that of T&O. These relations which, in the present approximation will be sufficient to conclude whether or not the series of inhomogeneous spheroids is stable, can be obtained as follows. The nine virial equations can be separated into two non-combining groups (see equations [20] to [23] and [26] to [30]), according to their parity with respect to the axis of rotation: an equation is odd if one, and only one, of the indices in the $L_{i;j}$'s that accompany it, is always a 3, whereas it is even if there are two indices, or none, with the value 3. Note that with the definitions

$$J_{11} \equiv I_{11}^n + [I_{11}^b - (\varepsilon + 1)^{-1} I_{11}^n], \quad (15)$$

$$J_{33} \equiv I_{33}^n + [I_{33}^b - (\varepsilon + 1)^{-1} I_{33}^n], \quad (16)$$

$$\langle \Omega \rangle J_{11} \equiv \Omega_n I_{11}^n + \Omega_a [I_{11}^b - (\varepsilon + 1)^{-1} I_{11}^n], \quad (17)$$

and

$$\langle \Omega^2 \rangle J_{11} \equiv \Omega_n^2 I_{11}^n + \Omega_a^2 [I_{11}^b - (\varepsilon + 1)^{-1} I_{11}^n], \quad (18)$$

and writing, for short, $\mathbf{W}_{sk;ij}$ instead of its detailed expression, our equations (20) to (23) and (26) to (30) have an entirely similar appearance to T&O's equations (27) to (30) and (36) to (40), respectively. More important is the fact that in the limit, $\varepsilon \rightarrow 0$ the frequencies of the Maclaurin spheroids (Ch 1969) are recovered intact from our dispersion relations and that, as in T&O's approach, neutral frequencies are found among the toroidal modes. In order to avoid the somewhat awkwardly expressions that would result if we were to write the definitions (15) to (18), and related expressions, in terms of ϵ_n and ϵ_a , as for example

$$\langle \Omega \rangle = \{ \Omega_n(\varepsilon + 1) + \Omega_a [\epsilon_n^5 \epsilon_a^{-5} (1 - \epsilon_a^2)^{1/2} (1 - \epsilon_n^2)^{-1/2} - 1] \} /$$

$$\{(\varepsilon + 1) + [\epsilon_n^5 \epsilon_a^{-5} (1 - \epsilon_a^2)^{1/2} (1 - \epsilon_n^2)^{-1/2} - 1]\}, \quad (19)$$

we will write our dispersion relations (with the one exception of that corresponding to the pulsation mode) in such a way that they look formally identical to T&O's ones, even if the meaning of corresponding terms is different. The names of the modes can be recalled realizing that when a Maclaurin spheroid is subjected to an arbitrary infinitesimal displacement, the virial equations odd in the index 3 allow to infer that the transverse cross-section at the equator remains undisturbed, while the neighbouring sections going north displace, say, to the right, with increasing amplitude the more we depart from the equator, reaching maximum amplitude at the pole. Since in the southern hemisphere the displacement is similar, but to the left, the name transverse-shear follows.

Similarly, from the equations even in the index 3 it can be shown that the infinitesimal perturbation turn the circular sections of the spheroid into ellipses—which axes do not coincide with the coordinate axes—rotating about the rotation axis. Finally, from the equations that yield the remaining mode one can infer that, while there occurs a deformation in the plane $x_i - x_j$, the poles oscillate vertically in opposite senses, thus producing a kind of pulsation.

2.3.1. The Transverse-Shear Modes

The four odd equations are:

$$\begin{aligned} & \lambda^2 \{I_{33}^n + [I_{33}^b - (\varepsilon + 1)^{-1} I_{33}^n]\} L_{1;3} - \{\Omega_n^2 I_{11}^n + \Omega_a^2 [I_{11}^b - (\varepsilon + 1)^{-1} I_{11}^n]\} L_{3;1} \\ &= (-2) \{ \{I_{33}^n (B_{13}^a + \varepsilon B_{13}^n) + [I_{33}^b - (\varepsilon + 1)^{-1} I_{33}^n] (B_{13}^a + \varepsilon B'_{13}^n)\} L_{1;3} \\ &+ \{I_{11}^n (B_{13}^a + \varepsilon B_{13}^n) + [I_{11}^b - (\varepsilon + 1)^{-1} I_{11}^n] (B_{13}^a + \varepsilon B'_{13}^n)\} L_{3;1} \}, \end{aligned} \quad (20)$$

$$\begin{aligned} & \lambda^2 \{I_{33}^n + [I_{33}^b - (\varepsilon + 1)^{-1} I_{33}^n]\} L_{2;3} - \{\Omega_n^2 I_{11}^n + \Omega_a^2 [I_{11}^b - (\varepsilon + 1)^{-1} I_{11}^n]\} L_{3;2} \\ &= (-2) \{ \{I_{33}^n (B_{13}^a + \varepsilon B_{13}^n) + [I_{33}^b - (\varepsilon + 1)^{-1} I_{33}^n] (B_{13}^a + \varepsilon B'_{13}^n)\} L_{2;3} \\ &+ \{I_{11}^n (B_{13}^a + \varepsilon B_{13}^n) + [I_{11}^b - (\varepsilon + 1)^{-1} I_{11}^n] (B_{13}^a + \varepsilon B'_{13}^n)\} L_{3;2} \}, \end{aligned} \quad (21)$$

$$\begin{aligned} & \lambda^2 \{I_{11}^n + [I_{11}^b - (\varepsilon + 1)^{-1} I_{11}^n]\} L_{3;1} + 2\lambda \{\Omega_n I_{11}^n + \Omega_a [I_{11}^b - (\varepsilon + 1)^{-1} I_{11}^n]\} L_{3;2} \\ & - \{\Omega_n^2 I_{11}^n + \Omega_a^2 [I_{11}^b - (\varepsilon + 1)^{-1} I_{11}^n]\} L_{3;1} \\ &= (-2) \{ \{I_{33}^n (B_{13}^a + \varepsilon B_{13}^n) + [I_{33}^b - (\varepsilon + 1)^{-1} I_{33}^n] (B_{13}^a + \varepsilon B'_{13}^n)\} L_{1;3} \\ &+ \{I_{11}^n (B_{13}^a + \varepsilon B_{13}^n) + [I_{11}^b - (\varepsilon + 1)^{-1} I_{11}^n] (B_{13}^a + \varepsilon B'_{13}^n)\} L_{3;1} \}, \end{aligned} \quad (22)$$

and

$$\lambda^2 \{I_{11}^n + [I_{11}^b - (\varepsilon + 1)^{-1} I_{11}^n]\} L_{3;2} - 2\lambda \{\Omega_n I_{11}^n + \Omega_a [I_{11}^b - (\varepsilon + 1)^{-1} I_{11}^n]\} L_{3;1}$$

$$\begin{aligned}
& -\{\Omega_n^2 I_{11}^n + \Omega_a^2 [I_{11}^b - (\varepsilon + 1)^{-1} I_{11}^n]\} L_{3;2} \\
& = (-2) \{ \{ I_{33}^n (B_{13}^a + \varepsilon B_{13}^n) + [I_{33}^b - (\varepsilon + 1)^{-1} I_{33}^n] (B_{13}^a + \varepsilon B_{13}^n) \} L_{2;3} \\
& \quad + \{ I_{11}^n (B_{13}^a + \varepsilon B_{13}^n) + [I_{11}^b - (\varepsilon + 1)^{-1} I_{11}^n] (B_{13}^a + \varepsilon B_{13}^n) \} L_{3;2} \} . \tag{23}
\end{aligned}$$

None of the equations (20) to (23) involves the variation in pressure and so, for these modes, it makes no difference whether the fluid is compressible or incompressible. The dispersion relation reads

$$\sigma^3 - 2\langle\Omega\rangle\sigma^2 + [\langle\Omega^2\rangle - (L + M)]\sigma + 2\langle\Omega\rangle M = 0 , \tag{24}$$

where

$$L = \mathbf{W}_{13;13}/J_{11} \quad \text{and} \quad M = \mathbf{W}_{31;13}/J_{33} , \tag{25}$$

and where the definitions (15) to (18) must be used. The roots from equation (24) are all real and different.

2.3.2. The Toroidal Modes

The five even equations are

$$\begin{aligned}
& \lambda^2 \{ I_{11}^n + [I_{11}^b - (\varepsilon + 1)^{-1} I_{11}^n] \} L_{1;1} + 2\lambda \{ \Omega_n I_{11}^n + \Omega_a [I_{11}^b - (\varepsilon + 1)^{-1} I_{11}^n] \} L_{1;2} \\
& \quad - 2 \{ \Omega_n^2 I_{11}^n + \Omega_a^2 [I_{11}^b - (\varepsilon + 1)^{-1} I_{11}^n] \} L_{1;1} \\
& = (-2) \{ \{ I_{11}^n [2B_{11}^a - a_{a_1}^2 A_{11}^a + \varepsilon(2B_{11}^n - a_{n_1}^2 A_{11}^n)] \\
& \quad + [I_{11}^b - (\varepsilon + 1)^{-1} I_{11}^n] [2B_{11}^a - a_{a_1}^2 A_{11}^a + \varepsilon(2B_{11}^n - a_{n_1}^2 A_{11}^n)] \} L_{1;1} \\
& \quad + \{ -I_{11}^n (a_{a_1}^2 A_{11}^a + \varepsilon a_{n_1}^2 A_{11}^n) - [I_{11}^b - (\varepsilon + 1)^{-1} I_{11}^n] (a_{a_1}^2 A_{11}^a + \varepsilon a_{n_1}^2 A_{11}^n) \} L_{2;2} \\
& \quad + \{ -I_{33}^n (a_{a_1}^2 A_{13}^a + \varepsilon a_{n_1}^2 A_{13}^n) - [I_{33}^b - (\varepsilon + 1)^{-1} I_{33}^n] (a_{a_1}^2 A_{13}^a + \varepsilon a_{n_1}^2 A_{13}^n) \} L_{3;3} \} \\
& \quad + P(L_{1;1} + L_{2;2} + L_{3;3}) , \tag{26}
\end{aligned}$$

$$\begin{aligned}
& \lambda^2 \{ I_{11}^n + [I_{11}^b - (\varepsilon + 1)^{-1} I_{11}^n] \} L_{2;2} - 2\lambda \{ \Omega_n I_{11}^n + \Omega_a [I_{11}^b - (\varepsilon + 1)^{-1} I_{11}^n] \} L_{2;1} \\
& \quad - 2 \{ \Omega_n^2 I_{11}^n + \Omega_a^2 [I_{11}^b - (\varepsilon + 1)^{-1} I_{11}^n] \} L_{2;2} \\
& = (-2) \{ \{ -I_{11}^n (a_{a_1}^2 A_{11}^a + \varepsilon a_{n_1}^2 A_{11}^n) - [I_{11}^b - (\varepsilon + 1)^{-1} I_{11}^n] (a_{a_1}^2 A_{11}^a + \varepsilon a_{n_1}^2 A_{11}^n) \} L_{1;1}
\end{aligned}$$

$$\begin{aligned}
& + \{I_{11}^n[2B_{11}^a - a_{a_1}^2 A_{11}^a + \varepsilon(2B_{11}^n - a_{n_1}^2 A_{11}^n)] \\
& + [I_{11}^b - (\varepsilon + 1)^{-1} I_{11}^n][2B_{11}^a - a_{a_1}^2 A_{11}^a + \varepsilon(2B'_{11}^n - a_{n_1}^2 A'_{11}^n)]\}L_{2;2} \\
& + \{-I_{33}^n(a_{a_1}^2 A_{13}^a + \varepsilon a_{n_1}^2 A_{13}^n) - [I_{33}^b - (\varepsilon + 1)^{-1} I_{33}^n](a_{a_1}^2 A_{13}^a + \varepsilon a_{n_1}^2 A'_{13}^n)\}L_{3;3}\} \\
& + P(L_{1;1} + L_{2;2} + L_{3;3}) , \tag{27}
\end{aligned}$$

$$\begin{aligned}
& \lambda^2 \{I_{33}^n + [I_{33}^b - (\varepsilon + 1)^{-1} I_{33}^n]\}L_{3;3} \\
& = (-2) \{ \{-I_{11}^n(a_{a_3}^2 A_{13}^a + \varepsilon a_{n_3}^2 A_{13}^n) - [I_{11}^b - (\varepsilon + 1)^{-1} I_{11}^n](a_{a_3}^2 A_{13}^a + \varepsilon a_{n_3}^2 A'_{13}^n)\}L_{1;1} \\
& + \{-I_{11}^n(a_{a_3}^2 A_{13}^a + \varepsilon a_{n_3}^2 A_{13}^n) - [I_{11}^b - (\varepsilon + 1)^{-1} I_{11}^n](a_{a_3}^2 A_{13}^a + \varepsilon a_{n_3}^2 A'_{13}^n)\}L_{2;2} \\
& \{I_{33}^n[2B_{33}^a - a_{a_3}^2 A_{33}^a + \varepsilon(2B_{33}^n - a_{n_3}^2 A_{33}^n)] \\
& + [I_{33}^b - (\varepsilon + 1)^{-1} I_{33}^n][2B_{33}^a - a_{a_3}^2 A_{33}^a + \varepsilon(2B'_{33}^n - a_{n_3}^2 A'_{33}^n)]\}L_{3;3}\} \\
& + P(L_{1;1} + L_{2;2} + L_{3;3}) , \tag{28}
\end{aligned}$$

$$\begin{aligned}
& \lambda^2 \{I_{11}^n + [I_{11}^b - (\varepsilon + 1)^{-1} I_{11}^n]\}L_{1;2} - 2\lambda \{\Omega_n I_{11}^n + \Omega_a [I_{11}^b - (\varepsilon + 1)^{-1} I_{11}^n]\}L_{1;1} \\
& - \{\Omega_n^2 I_{11}^n + \Omega_a^2 [I_{11}^b - (\varepsilon + 1)^{-1} I_{11}^n]\}(L_{1;2} + L_{2;1}) \\
& = (-2) \{ \{I_{11}^n(B_{11}^a + \varepsilon B_{11}^n) \\
& + [I_{11}^b - (\varepsilon + 1)^{-1} I_{11}^n](B_{11}^a + \varepsilon B'_{11}^n)\}(L_{1;2} + L_{2;1}) \} , \tag{29}
\end{aligned}$$

and

$$\begin{aligned}
& \lambda^2 \{I_{11}^n + [I_{11}^b - (\varepsilon + 1)^{-1} I_{11}^n]\}L_{2;1} + 2\lambda \{\Omega_n I_{11}^n + \Omega_a [I_{11}^b - (\varepsilon + 1)^{-1} I_{11}^n]\}L_{2;2} \\
& - \{\Omega_n^2 I_{11}^n + \Omega_a^2 [I_{11}^b - (\varepsilon + 1)^{-1} I_{11}^n]\}(L_{1;2} + L_{2;1}) \\
& = (-2) \{ \{I_{11}^n(B_{11}^a + \varepsilon B_{11}^n)
\end{aligned}$$

$$+[I_{11}^b - (\varepsilon + 1)^{-1} I_{11}^n](B_{11}^a + \varepsilon B'^{n}_{11})\}(L_{1;2} + L_{2;1})\} . \quad (30)$$

We can obtain a homogeneous system of two equations, in the unknowns $(L_{1;1} - L_{2;2})$ and $(L_{1;2} + L_{2;1})$, by subtracting equation (27) from equation (26), and adding equations (29) and (30). From such system there results the dispersion relation

$$(2N - 2\langle\Omega^2\rangle - \sigma^2)^2 - 4\langle\Omega\rangle^2\sigma^2 = 0 , \quad (31)$$

where

$$N = W_{12;12}/J_{11} , \quad (32)$$

the other quantities having their usual meaning. Once again, the change in pressure has been eliminated so that the same remarks in regard to equation (24) apply here. The roots that equation (31) yield are largely real; nevertheless, complex roots and, moreover, neutral modes are also possible.

2.3.3. The Pulsation Mode

In view of the dependence on the compressibility of T&O's dispersion relation for the pulsation mode, it is evident that their approach is no longer useful to us. On the other hand, we need a homogeneous system of equations free from the variation in pressure which includes equation (28) since, so far, this equation remains unused. To this end, we add equations (26) and (27) and to the resulting equation subtract twice equation (29). In order to exclude solutions (31) and remain consistent with equations (26) to (30) we set

$$L_{1;1} = L_{2;2}$$

and

$$L_{1;2} = -L_{2;1} . \quad (33)$$

Next, we subtract equation (29) from equation (30), exclude the root $\lambda = 0$, and use the divergence relation

$$L_{k;k} = \partial\xi_k/\partial x_k = 0 , \quad (34)$$

required by the solenoidal character of $\vec{\xi}$ (Ch 1969). The dispersion relation obtained from the above procedure is

$$R\sigma^2 + S = 0 , \quad (35)$$

where

$$R = 1/2 + (1 - \epsilon_a^2) , \quad (36)$$

and

$$\begin{aligned} S = & \langle\Omega^2\rangle - (1/2)(\mathbf{W}_{11;11} + \mathbf{W}_{11;22} - 2\mathbf{W}_{11;33})/J_{11} \\ & +(1 - \epsilon_a^2)(\mathbf{W}_{33;11} - \mathbf{W}_{33;33})/J_{33} . \end{aligned} \quad (37)$$

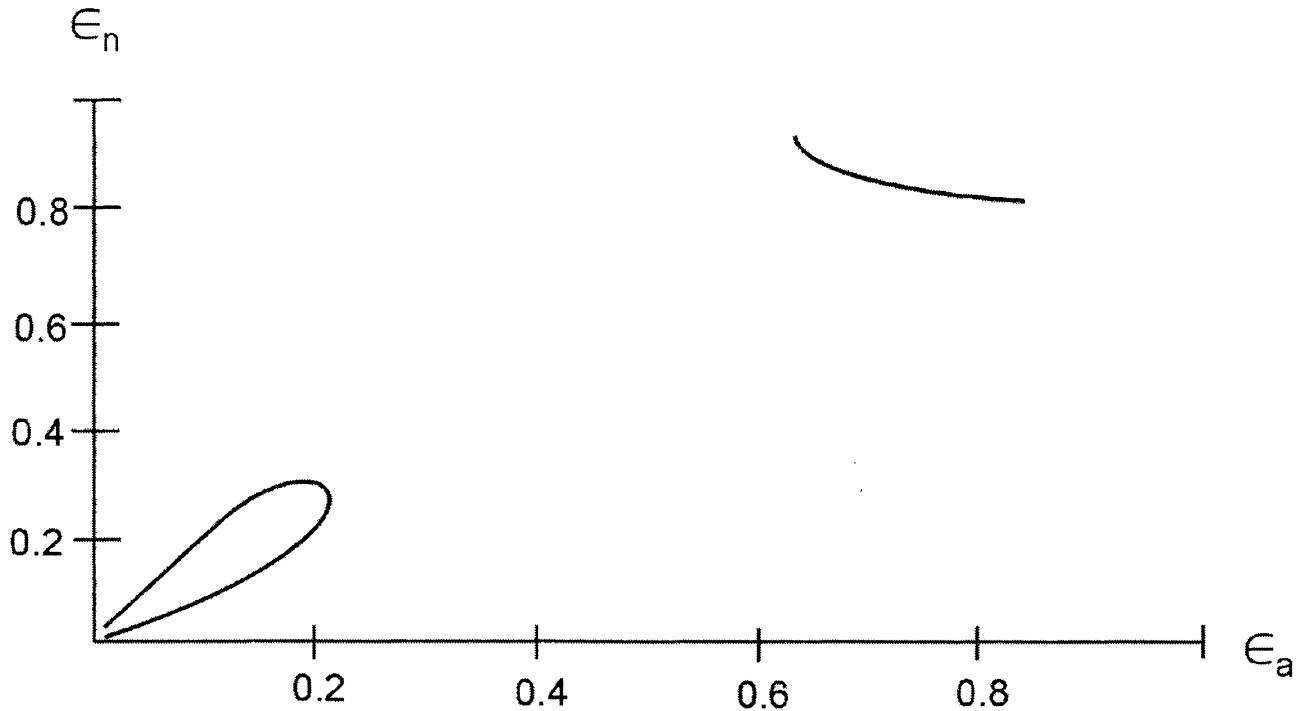


Fig. 3. The behavior of ϵ_n as a function of ϵ_a of the bifurcation points for $\varepsilon = 5$, according to Table 2.

For the evaluation of the second term of the right-hand side of equation (37), we use a property of the supertensor of potential energy (Ch 1969, equation [150], Chapter 3). The roots from equation (35) are all real.

3. NUMERICAL RESULTS

The body's characteristic frequencies of oscillation will now be considered. To this end, the series will be presented in subfamilies of fixed ε , as in Table 1. Each subfamily begins at a low ϵ_a value and then ϵ_n is let to run through increasing values; next, the procedure is repeated for a larger ϵ_a value, and so forth. Table 1, which contains data ranging from $\varepsilon = 0.5$ up to $\varepsilon = 50$ can be read as follows: column 1 gives ϵ_n ; columns 2 and 3 give the angular velocities of the nucleus and the atmosphere; the oscillation modes normalized to $\sqrt{2\pi G\rho_a}$ (columns 4 to 9) are called $\sigma_1, \sigma_2, \sigma_3$ (transverse-shear), σ_4, σ_5 (toroidal), and σ_6 (pulsation). We will focus attention on columns 7 and 8, the toroidal modes, where the main features of the current problem arise.

3.1. The Instability Gaps

The discernment of instability along the series is provided by the occurrence of complex roots out of equation (31). Otherwise the series is stable, since the roots from equations (24) and (35) are always real. Columns 7 and 8 of Table 1 show narrow ranges of ϵ_n where complex roots occur for various ϵ_a values; in each case instability sets in at the value where the complex gap initiates, Complex_i , and continues prevailing up until the complex gap finalizes, Complex_f , beyond which stability resumes. The spheroids within these gaps are therefore unstable, and are usually either of very low or very high ϵ_a and ϵ_n . Instability also depends strongly on the body's degree of inhomogeneity ε . The distribution of the complex gaps among the series seen according to increasing ε is roughly as follows: instability gaps of low (about 0.1) ϵ_a and ϵ_n occur only up to ε about 25, to thereafter disappear altogether. Gaps of high (about 0.98) ϵ_a and ϵ_n , which are not initially present, appear for the first time for ε about 5, and remain thereafter. To illustrate the case of extremely high ε let us take $\varepsilon = 1000$ (not included in Table 1), for which complex gaps occur through almost the full range of ϵ_a for ranges of ϵ_n initiating at about 0.9. The spheroids of $\varepsilon = 1000$ of ϵ_a lower than about 0.15 are stable

TABLE 1 (CONTINUED)

ϵ_n	Ω_n^2	Ω_a^2	$(-) \sigma_1$	σ_2	σ_3	σ_4	σ_5	$(\pm) \sigma_6$
0.81599	9.59810	3.68188	4.0281	3.0572	7.0928	$\sim 10^{-8}$	6.1218	4.5529
0.9	11.2425	2.1299	3.6797	3.1204	6.9423	1.1506	5.2323	4.4553
$\epsilon_a = 0.8$								
0.81271	9.53868	8.59123	4.0491	3.0881	7.1372	$\sim 10^{-7}$	6.1762	4.4963
0.85	10.3358	6.8271	3.9810	3.2082	7.1900	0.4932	5.9240	4.5973
0.9	11.2283	4.8140	3.8341	3.3094	7.1612	1.2804	5.3560	4.7094
$\epsilon_a = 0.8125$								
0.81267	9.54280	9.52940	4.0487	3.0891	7.1378	$\sim 10^{-10}$	1.7807	6.2693
$\epsilon_a = 0.9$								
0.95	11.3034	6.9283	3.5941	3.3459	6.9489	2.7803	3.9205	4.5350
0.9544	11.2097	6.5453	3.5539	3.3269	6.8941	Complex _i		4.5359

^aWe use the following notation: $\epsilon + 1$ is the density ratio $\rho_n \rho_a^{-1}$; Ω^2 refers to squared angular velocity normalized to $2\pi G \rho_a$; ϵ_n , ϵ_a , are the eccentricities of the nucleus and the atmosphere, respectively; σ is the frequency normalized to $\sqrt{2\pi G \rho_a}$; subscripts in σ are used as follows: 1, 2, 3 for the transverse-shear modes, 4, 5 for the toroidal modes, and 6 for the pulsation mode. Complex_i signals the point where instability sets in. Stability resumes beyond the point Complex_f. Points of bifurcation are given with an extra figure in the three first columns.

for any value of ϵ_n . Accordingly, one can roughly expect that real rotating stars would turn unstable if their density ratio is moderate ($\epsilon \cong 25$) and their flattenings low ($\epsilon_{n,a} \cong 0.1$), but also if the flattenings are large and the density ratio is from moderate to high.

3.2. The Bifurcated Ellipsoids

In addition to the instability gaps, relation (31) also generates neutral modes—neutral toroidal modes are also present in T&O’s work—meaning that within the series some spheroids are of zero frequency, i.e., they become permanently deformed by the perturbation. The occurrence of the neutral spheroids vary widely with ϵ , and are discretely distributed within a given subfamily, so that for given ϵ_a there is only one of these spheroids for a certain ϵ_n value. Otherwise, for varying ϵ_a we have instead a continuous gap of neutral spheroids, whose initial and final values are quoted in Table 1 in single, separate rows. For example, for $\epsilon = 5$, isolated neutral spheroids occur for ϵ_n values as low as 0.10169 and as large as 0.81267. For varying ϵ_a however, we have neutral spheroids in two different continuous ranges: $0.1 < \epsilon_a < 0.21$ and $0.68 < \epsilon_a < 0.8125$; in-between these ranges neutral spheroids are not found for this particular ϵ value. The lower portion of the quoted range is double-valued: for a given ϵ_a , there are two different ϵ_n , one value being about equal to its corresponding ϵ_a , the other one being relatively larger. The upper portion is, however, single-valued. Table 2 is intended to come off with these aspects of the neutral spheroids, which may not show off clearly in Table 1.

Figure 3 illustrates the behavior of ϵ_n as a function of ϵ_a for this example, the curve showing clearly both, its double-valued as well as its single-valued portions.

For ϵ larger than about 35, the double-valued portion of the ϵ_a vs ϵ_n curve disappears altogether, while the single-valued portion stretches steadily over its left. For $\epsilon = 1000$, the single-valued portion stretches down to $\epsilon_a = 0.2$.

Since secondary sequences of triaxial figures are expected to branch off, or bifurcate, from spheroids of zero frequency we will, following Chandrasekhar, refer to them as points of bifurcation. As for our analysis, ellipsoidal configurations are indeed found to bifurcate from such points but we hasten to add that they do not rotate as a solid-body rather; they are static with internal motions of differential vorticity, the vorticity of the nucleus being always larger than that of the atmosphere. The figures of the bifurcated sequences are ellipsoids even though this geometry shows off more clearly by the nucleus in both the equatorial and polar directions.

TABLE 2
RANGES OF ϵ_n AND ϵ_a FOR POINTS OF BIFURCATION,
FOR $\epsilon = 5^a$

ϵ_a	ϵ_n	ϵ_a	ϵ_n	ϵ_a	ϵ_n
0.06	0.06034	0.16	0.16846	0.68	0.90250
	0.14993		0.25113		
0.08	0.08083	0.18	0.19367	0.70	0.86723
	0.17771		0.26125		
0.10	0.10169	0.20	0.22334	0.75	0.82631
	0.20109		0.26567		
0.12	0.12307	0.21	0.24520	0.80	0.81334
	0.22089		0.26045		
0.14	0.14519			0.8125	0.81267
	0.23753				

^aThe splitting into two of the ϵ_n values in the lower part of the total range is because this part of the ϵ_a range is double-valued.

As for the equatorial flattening of the atmosphere, it is consistently very low whether the nucleus is a well-defined or a poorly defined ellipsoid. For ellipsoids whose nucleus have equatorial flattening larger than 0.1, the polar flattening of the nucleus (atmosphere) is always very high (very low), so that the atmospheres are nearly spherical, with only slight vestiges of ellipticity. Thus, the overall shape of one of these figures is like that of a small massive seed embedded within a tenuous spherical atmosphere. The relative shape of the last figures of a given sequence of ellipsoids is explained by the fact that the vorticity of the nucleus is very much larger than that of the atmosphere which, in addition, is close to zero.

The just described Dedekind-type inhomogeneous figures had been independently calculated in a previous work (Cisneros et al. 1995), where they were distinguished as spheroids, figures of transition, and ellipsoids, depending if their nucleus had a low moderate or high equatorial flattening. Here we do not use such distinction and call all the figures simply ellipsoids. The parameters of the ellipsoids for $\epsilon = 5$ are given in Table 3; the first row represents the “best” spheroid attained by our calculation that fits into the values of the bifurcation spheroid, as taken from Table 1. Here, Z^2 refers to squared vorticity normalized to $4\pi G\rho_a$; ϵ_{n_1} , ϵ_{a_1} , ϵ_{n_2} , ϵ_{a_2} are the equatorial (1) and meridional (2) eccentricities of the nucleus (n) and the atmosphere (a). Column 2 gives the equatorial flattening of the nucleus for increasing ϵ_{n_1} values, ranging from 0.0001 up to 0.9. For fixed ϵ , we find that all the sequences converge to the same ellipsoids, independently of which spheroid of bifurcation we depart from. Actually, for same ϵ_n and different ϵ , only the vorticity Z_n^2 clearly distinguishes one ellipsoid of another.

Note that the last point of bifurcation for every subfamily occurs for $\epsilon_a = 0.8125$ and $\epsilon_n = 0.8127$; this figure would then correspond to the last point of the single-valued portion of the curve shown in Figure 3. This spheroid is of particular interest because, in spite of the fact that $\rho_n > \rho_a$ and $\omega_n > \omega_a$, it has a nucleus that has grown up in such a way that occupies practically the volume of the whole body so, in this sense, becoming homogeneous. Indeed, the Jacobi, and so the Dedekind, series branches off the Maclaurin series at $\epsilon = 0.81267$.

4. SUMMARY AND CONCLUSIONS

The aim of the current work has been to study the stability of a model made up of two confocal spheroids with differential solid-body rotation, previously established as a series of equilibrium configurations. In so doing, we confronted the somehow unexpected result that spheroids of neutral frequency (therefore, becoming permanently deformed in the chosen inertial frame) are found among the general solution, so that ellipsoids branch off from such a model, in much the same way as the Jacobi sequence branches off the Maclaurin sequence. A fundamental difference with that classic result is that the bifurcated inhomogeneous ellipsoids at

TABLE 3
PROPERTIES OF THE STATIC ELLIPSOIDS, FOR $\varepsilon = 5^a$

Z_n^2	ϵ_{n_1}	ϵ_{n_2}	$10^4 Z_a^2$	$10^4 \epsilon_{a_1}$	ϵ_{a_2}
$\varepsilon = 5$					
2.4819	0.0001	0.8672	7754.2	0.8050	0.6980
2.4899	0.0002	0.8680	6336.2	1.5400	0.6678
2.4925	0.0003	0.8682	5891.5	2.2700	0.6568
2.4995	0.0004	0.8688	5122.6	2.9270	0.6357
2.5202	0.0005	0.8692	2881.0	2.9600	0.5147
2.6564	0.0006	0.8876	637.4	2.1900	0.3244
2.6676	0.0007	0.8887	470.5	2.2400	0.2844
2.6766	0.0008	0.8890	262.6	1.9600	0.2174
2.6838	0.0009	0.8897	165.7	1.7600	0.1744
2.6873	0.0010	0.8900	112.1	1.6200	0.1440
2.5284	0.0025	0.8570	41.6	2.6000	0.0881
2.5326	0.0050	0.8578	35.5	4.8000	0.0814
2.5284	0.0075	0.8568	18.5	5.1480	0.0588
2.5319	0.0100	0.8573	2.9	2.7500	0.0236
2.5313	0.0250	0.8572	2.4	6.2600	0.0215
2.5317	0.0500	0.8574	0.3	4.4000	0.0075
2.5317	0.0750	0.8577	0.2	6.0000	0.0068
2.5318	0.1000	0.8580	0.1	6.6000	0.0057
2.5325	0.2000	0.8604	0.1	11.190	0.0048
2.5361	0.3000	0.8645	0.08	12.597	0.0036
2.5466	0.4000	0.8704	0.07	15.350	0.0033
2.5724	0.5000	0.8785	0.063	16.970	0.0030
2.6302	0.6000	0.8894	0.084	22.147	0.0033
2.7589	0.7000	0.9039	0.080	23.740	0.0030
3.0707	0.8000	0.9235	0.093	27.32	0.0031
4.0864	0.9000	0.9516	0.101	31.09	0.0033

^aWe use following notation: $\epsilon + 1$ is the density ratio $\rho_n \rho_a^{-1}$; Z^2 refers to squared vorticity normalized; $\epsilon_{n_1}, \epsilon_{a_1}, \epsilon_{n_2}, \epsilon_{a_2}$ are the equatorial (1) and meridional (2) eccentricities of the nucleus (n) and the atmosphere (a). The ϵ_{n_2} and ϵ_{a_2} values of the first ellipsoid of each sequence corresponds to the spheroid of neutral frequency, or bifurcation point (taken from Table 1), while ϵ_{n_1} is the lowest attainable value that, according to our calculations, fits into such spheroid.

hand are actually static, Dedekind-type, with internal motions of differential vorticity (and so Hamy's theorem is respected). The current work also helped to establish these ellipsoids as exact equilibrium figures, rather than only approximate, as was originally introduced (Cisneros et al. 1995). Since the solution to our problem confined the unstable models to easily located regions we may—in the considered approximation—conclude that the rest of the figures of the series are stable and, consequently, are permanent figures. It remains, of course, to drop the condition of continuity over the $L_{i;j}$'s across the boundary nucleus-atmosphere, and to extend to third order the calculations. Also, it remains to test the static ellipsoids for stability.

REFERENCES

- Chambat, F. 1994, A&A, 292, 76
Chandrasekhar S 196 Ellipsoids Figure O Equilibrium (Yale: University Press)
Chandrasekhar, S., & Lebovitz, N. R. 1962, ApJ, 135, 248
Cisneros, J., Martínez, F. J., & Montalvo, D. 1995, RevMexAA, 31, 101
Hamy, M. 1887, Etude sur la Figure des Corps Célestes, Thése de la Faculté des Sciences, Annales de l'Observatoire de Paris, 1889, Mémoires, 19
Landau, L. D., & Lifshitz, E. M. 1959, Course of Theoretical Physics: Fluid Mechanics (New York: Pergamon Press)
Montalvo, D., Martínez, F. J., & Cisneros, J. 1983, RevMexAA, 5, 293
Tassoul, J. L., 1978, Theory of Rotating Stars (Princeton: Princeton Univ. Press), 82
Tassoul, J. L., & Ostriker, J. P. 1968, ApJ, 154, 613

J. U. Cisneros Parra: Facultad de Ciencias, Universidad Autónoma de San Luis Potosí, Alvaro Obregón No. 64, 78000 San Luis Potosí, S. L. P., México (cisneros@galia.fc.uaslp.mx).

F. J. Martínez Herrera and J. D. Montalvo Castro: Instituto de Física, Universidad Autónoma de San Luis Potosí, Alvaro Obregón No. 64, 78000 San Luis Potosí, S. L. P., México.